Improved beta (local beta > 1) and density in electron cyclotron resonance heating on the RT-1 magnetosphere plasma

M. Nishiura[1], Z. Yoshida[1], H. Saitoh[1], Y. Yano[1], Y. Kawazura[1], T. Nogami[1], M. Yamasaki[1], T. Mushiake[1], A. Kashyap[1]

[1]Graduate School of Frontier Sciences, The University of Tokyo, Kashiwanoha, Kashiwa, Chiba, 277-8561 Japan

E-mail contact of main author: nishiura@ppl.k.u-tokyo.ac.jp

Abstract

This study reports the recent progress in improved plasma parameters of the RT-1 device. Increased input power and the optimized polarization of electron cyclotron resonance heating (ECRH) with an 8.2 GHz klystron produced a significant increase in electron beta, which is evaluated by an equilibrium analysis of Grad-Shafranov equation. The peak value of the local electron beta β_e was found to exceed 1. In the high beta and high-density regime, the density limit was observed for H, D, and He plasmas. The line average density was close to the cutoff density for 8.2 GHz ECRH. When the filling gas pressure is increased, the density limit still exists even at the low beta region. This result indicates the density limit is caused by the cutoff density rather than the beta limit. From the analysis of interferometer data, we found that inward diffusion causes a peaked density profile beyond the cutoff density.

1. Introduction

The ring trap 1 (RT-1) device is a "laboratory magnetosphere" created by a levitated superconducting ring magnet, which is dedicated to studying of physical processes in the vicinity of a magnetic dipole. A strongly inhomogeneous magnetic field gives rise to interesting plasma phenomena such as inward diffusion and self-organized confinement which are

degenerate in homogeneous (or zero) magnetic fields [1]. The RT-1 experiment has demonstrated the self-organization of a plasma clump with a steep density gradient; a peaked density distribution is spontaneously created through "inward diffusion" [2-4]. Inward diffusion is known to occur in stellar magnetospheres [5]. The idea of dipole confinement to simulate a magnetosphere in a laboratory system was first proposed by Hasegawa [6]. The LDX experiment is also exploring high-beta confinement by a dipole system [7]. They observe that peaked density profile is created by turbulence-driven inward diffusion [8].

When the local electron beta β_e in the RT-1 is close to 0.7 [9], the ions remain cold being virtually decoupled with the hot component (> 10 keV) and low density (< 10^{18} m^{-3}) electrons. For advanced fusion researches, although we require higher ion temperature, density, and plasma pressure, the ion temperature of the RT-1 is still situated in the linear regime.

When the ion temperature increases further, two-fluid effects on the plasma flow is expected to appear theoretically in a high ion beta plasma ($\beta_i \geq 0.1$) and nonlinear regime (the Bernoulli-Beltrami state) [9]. Thus two scenarios are investigated to realize the ion heating. Scenario A is to conduct an ion cyclotron resonance heating (ICRH). Scenario B is to prompt a collision relaxation between hot electrons and ions. The increased density is a better direction to a collision relaxation as well as an antenna coupling of ICRH. In both cases, achieving an electron density > 10^{18} m^{-3} as a target plasma is essential. The RT-1 was implemented with an 8.2 GHz klystron for electron cyclotron resonance heating (ECRH) that can inject the power of 25 kW per a transmission line. The recent upgrade in adding a transmission line extends the accessible regime in electron density and diamagnetism which corresponds to β_e [10]. This paper describes the extension of the operation regime during the ECRH experiments for Scenario B. The cutoff density of 8.2 GHz electromagnetic wave is 8.4×10^{17} m^{-3}. The line average density is limited by the cutoff density, although the filling gas pressure is scanned with keeping the ECRH power.

2. Electron cyclotron heating in RT-1

Fig. 1 shows the top view and cross section of the RT-1 device. The levitated superconducting coil is located at the mid plane (z = 0) during plasma experiments. The plasma is produced and sustained by ECRH which consists of an 8.2 GHz klystron with 100 kW and the pulse length of 1 second. The full power injection using the transmission lines L#1 and L#2 is restricted at 25 kW per a transmission line because of the heat endurance of a vacuum-seal window and a breakdown in the waveguides. The existing ECRH transmission line L#1 was used, and the new line L#2 has been recently added by inserting a power divider on the original transmission line. The new transmission line increases the total ECRH power on RT-1 from 25 kW to 50 kW. The EC beams are directed to the ECR layer located on their ways from the upper ports, and travel through the plasma edge region. The fundamental ECR layer exists at 0.293 T for 8.2 GHz.

The 75 GHz interferometers measure the line average electron density $\bar{n}_e$ at the tangency radius of 0.45 m, and vertically at the radii of 0.6 and 0.7 m. The measured $\int n_e \, dl$ at the centre chord (0.45m) is divided by 1.6 m that corresponds to the distance across the plasma inside the separatrix in a vacuum magnetic field, and thus $\bar{n}_e$ is used as the line average electron density. Four loop antennae measure the diamagnetic signal W_p that are averaged. The typical waveforms of the ECRH power, W_p and $\bar{n}_e$ are plotted in Fig. 2. In this case, the transition in W_p to a high beta state is appeared at t = 1.142 s. The phenomena usually occurs above a threshold of ECRH power, but independently of filling gas species. Fig. 3 shows the dependence of ECRH power on the diamagnetic signal. The diamagnetic signal increases up to 40 kW. This result indicates the ECRH power is absorbed effectively to plasmas. Although the hydrogen gas pressure is varied from 3.8 to 13 mPa, the change in the diamagnetic signal is a

slight level at the same ECRH power. The diamagnetic signal under the levitated coil operation improves clearly by an order of magnitude compared with the supported coil operation.

3. Extended operation regime in RT-1

The operation regime of the RT-1 device was investigated and was extended to a higher electron density and beta value [10], which are indicated as the "conventional operation regime" (see Fig. 4). The EC waves were injected as both O-modes for two launchers L#1 and L#2 in the conventional operation regime. For further extended regime, the polarizations of EC waves for two launchers L#1 and L#2 were investigated to optimize the deposition and heating efficiency. A twisted waveguide was inserted in the transmission line to rotate the polarization direction of 90 degrees from O- to X-modes. A rectangular horn antenna with 128×105 mm opening and 170 mm in length is attached to the L#1 port to improve a beam focusing. In the case of L#1 X-mode and L#2 O-mode injections at the ECRH power of 50 kW, W_p increases by approximately 10%, and $\bar{n}_e$ increases by 30%, compared with the conventional operation regime. The core chord of the interferometer reaches the maximum $\bar{n}_e = 6.9\times10^{17}$ m^{-3} for H, 7.5×10^{17} m^{-3} for D, and 8×10^{17} m^{-3} for He at the input power of 40 kW. In the case of both L#1 and L#2 X-modes, the achievable $\bar{n}_e$ improves slightly with no observable increase in W_p. The broken line indicates the cutoff density of 8.2 GHz EC wave. The helium discharge achieved around the cutoff density at 15 kW. $\bar{n}_e$ for all discharges remains below the cutoff density even though the input power of ECRH is increased to more than 40 kW. To achieve higher line average density, the filling gas pressure is increased. When a gas pressure is set, the ECRH power is gradually increased from ~10 to 45 kW. The diamagnetism is increased, when the input power increases. The maximum diamagnetism reaches to the maximum at H_2 gas pressure of 17 mPa. When the gas pressure is increased to 38 mPa, the diamagnetism decreases

to 4 mWb. The further increase of the gas pressure decreases the diamagnetism. In the case of He discharge, the maximum diamagnetism is 5.2 mWb at He gas pressure of 11 mPa. When the He gas pressure is increased to 15 and 29 mPa, the diamagnetism and the electron density decrease to 2 mWb at $7.9\text{x}10^{17}\text{m}^{-3}$, and 0.8 mWb at $6\text{x}10^{17}\text{m}^{-3}$, respectively. The dependence of the diamagnetism and the electron density on He gas pressure is the same tendency for H_2 gas.

In the high beta regime that we attained in the experiments, the maximum W_p was 5.9 mWb for H. The lower bound of β_e is estimated by the equilibrium analysis of Grad-Shafranov equation. The fitting function from magnetic measurements at nine positions was used as an initial guess for the solution. Here the lower bound is given by the extrapolation of the linear relation $\beta_e = 18\ W_p$ that holds in the regime of $W_p < 3$ mWb. In the higher beta regime, the nonlinear effect of the self-magnetic field diminishes W_p, thus the linear relation underestimates the beta. The possible anisotropic electron pressure (due to resonance heating of the perpendicular component) also produces an underestimate of the beta in the MHD fitting [11]. From this analysis, the local β_e was found to exceed 1 at $W_p = 5.9$ mWb.

The high-beta plasma in a dipole magnetic field is characterized by a strongly peaked density profile [3, 4, 8], which is explained by a kinetic equilibrium theory [4, 11]. In the high-density regime for $\bar{n}_e = 7.8\times10^{17}$ m^{-3} in the He plasma, the density profile was reconstructed in Fig. 5 from three-chord interferometer-data. The method to obtain a 2D density profile is described in [10]. The highest position of electron density is located at the outer side of the levitation coil. Even though the density limit exists in $\bar{n}_e$ as seen in Fig. 4, the 2D profile of electron density forms a central peaking, which exceeds the cutoff density of 8.2 GHz-ECRH; hence, the peaked density ($> 10^{18}$ m^{-3}) is produced by uphill diffusion. The analysis assumes the density profile as a function of r^{-a} at z = 0. Here "a" is a constant estimated by the fit. It

is found that the electron density at the peak would exceed the cutoff density except for a flat or an anisotropic profile.

The isotope effect of H and D plasmas was investigated at the ECRH power of 40 kW (see Fig. 4). The W_p shows no clear difference between H and D plasmas, and $\bar{n}_e$ for the D plasma increases 8%. The isotope effect does not show a drastic enhancement of the plasma performance in this operation regime.

In the high density regime, the electron density fluctuation level was measured because it might be related to the density and beta limit. The interferometers observe fluctuations in the electron density which has a discrete spectrum of cascade modes at frequencies less than 1 kHz. The fluctuation is spatially localized in the edge of the confinement region. Although the fluctuations induced by instabilities result in a plasma disruption of Tokamak plasmas, the observed fluctuations do not provoke a disruption of the produced plasma. The reflectometer with the frequency of 3.9 GHz also measures the density fluctuation from outboard side at z = 0 mid-plane of RT-1. Fig. 6 shows the fluctuation level measured for H, D, and He plasmas. The fluctuation level for He plasmas is highest compared with those for H and D plasmas. When $\bar{n}_e > 6\times10^{17}$ m^{-3} at the He gas pressure of 12 and 30 mPa, the fluctuation level increases obviously. From the electron density profile, the reflection position shifts to the outer radial position as the electron density is higher. The observed fluctuation level is strongly related to the radial position of reflection rather than the growth of instabilities in these experiments.

4. Impurity ions and non-thermal electrons from x-ray spectra

The x-ray spectra were measured by a Si-PIN phodiode detector (XR-100CR, Amptek). The measured data were accumulated during 1 sec discharges. The detector viewed the plasma through a Be window with 12.5 μm thickness at the radial location of 0.7 m with a vertical

sightline. The Be window eliminates a light emission from plasmas. The transmittance of Be window are corrected to obtain an intensity of x-ray spectrum from photon counting.

The characteristic x-rays from impurities are observed in the case of low density operation (~2×10^{17}m^{-3}), while they are below the bremsstrahlung radiation in the case of high density operation (~7×10^{17}m^{-3}). The Kα and Kβ lines in x-ray spectra were noticeable for Cr (5.41 and 5.95 keV) and Fe (6.40 and 7.06 keV), respectively. These characteristic x-rays would be produced by the collision of high energy electrons with inside structures (the stainless surface of the vacuum chamber, the centre stack, and the support rods of levitating coil) of RT-1.

The electron temperature T_{eh} was obtained by a fitting function [12, 13] from the measured x-ray spectra

$$\mathrm{I}(h\nu) = h\nu\frac{dn}{dh\nu} \propto \frac{1}{\sqrt{T_{eh}}} exp\left(-\frac{h\nu}{T_{eh}}\right)$$

where $h\nu$ is the photon energy, and dn is the photon count number in the photon energy interval $dh\nu$, and I is the power radiated in a unit volume. Although more precise fitting function is required to obtain accurate T_{eh}, other factors (Gaunt factor, effective charge, and electron and ion densities) are assumed to be a constant for convenience. Fig. 7 shows the dependence of high energy component of electrons on the ECRH power in hydrogen plasmas at the gas pressure of 7.6 mPa. T_{eh} increases from 16 keV to 30 keV as the input ECRH power P_{ECRH} is increased. For the fixed ECRH power of 45 kW, T_{eh} and W_p are plotted as a function of the line average density in Fig. 8. The helium gas pressure is increased to produce higher electron density in the same operation range as in Fig. 4. Near the cutoff density $\bar{n}_e$~ 0.8×10^{18} m^{-3}, T_{eh} and W_p decrease with the increase of filling gas pressure. The heating efficiency at the ECR layer would be reduced due to the cutoff density. To understand the absorption of EC wave, the optical depth for 8.2 GHz fundamental resonance is calculated, based on the reference [14]. Our results for 8.2 GHz case have the same tendency as those in Fig. 4.4 of [14]. It is found that the

shallow angle injection corresponding to the magnetic field enhances the optical depth for X-mode wave, compared with O-mode wave from the calculated results. The perpendicular injection for X-mode reduces one pass absorption, but it increases the cutoff density at the ECR layer. The improvement of the heating efficiency is one of the possibilities that can explain the extended operation regime of the local β_e and $\bar{n}_e$.

5. Conclusion

The upgrade and optimization in ECRH system extended the operation regime in electron beta and electron density in the magnetosphere plasmas in RT-1. The local β_e was found to exceed 1 from the solution of Grad-Shafranov equation. The density limit appears in the experiments, when the line average density at the tangency radius of 0.45 m is close to the cutoff density for 8.2 GHz EC wave. Then the electron density profile reconstructed from the interferometers provides the peaked profile beyond the cutoff density. The phenomena is explained by the inward diffusion that is described in [4]. During ECRH experiments x-ray spectra in the range from 10 to 50 keV were obtained in RT-1. The temperature of high energy electrons decreases as the electron density increases. Ions still remained low temperature under ECRH experiments. In higher ion temperature (~ion beta), a nonlinear phenomenon (diverse structures in plasmas) is considered to emerge theoretically [9]. The electron density of higher than 10^{18} m^{-3} improve the coupling between the ion cyclotron antenna and plasmas, and it leads to an effective ion heating to realize higher ion beta condition.

Acknowledgment

Authors would like to thank Dr. Furukawa of Tottori University for discussion. This work was supported by JSPS KAKENHI Grant Numbers 23224014 and 24360384.

6. References

[1] Yoshida, Z., Mahajan, S. M., Prog. Theor. Exp. Phys. (2014) 073J01.

[2] Yoshida, Z., Saitoh, H., Morikawa, J., Yano, Y., Watanabe, S., Ogawa, Y., Phys. Rev. Lett. **104** (2010) 235004.

[3] Saitoh, H., Yoshida, Z., Morikawa, J., Yano Y., Mizushima, T., Ogawa, Y., Furukawa, M., Kawai, Y., Harima, K., Kawazura, Y., Kaneko, Y., Tadachi, K., Emoto, S., Kobayashi, M., Sugiura, T., Vogel, G., Nucl. Fusion **51** (2011) 063034.

[4] Yoshida, Z., Saitoh, H., Yano, Y., Mikami, H., Kasaoka, N., Sakamoto, W., Morikawa, J., Furukawa, M., Mahajan, S. M., Plasma Phys. Control. Fusion **55** (2013) 014018.

[5] Schulz, M., Lanzerotti, L. J., *Particle Diffusion in the Radiation Belts* (Springer-Verlag, Berlin Heidelberg New York, 1974).

[6] Hasegawa, A., Chen, L., Mauel, M. E., Nucl. Fusion **30** (1990) 2405.

[7] Garnier, D. T., Boxer, A. C., Ellsworth, J. L., Kesner, J., Mauel, M. E., Nucl. Fusion **49** (2009) 055023.

[8] Boxer, A. C., Bergmann, R., Ellsworth, J. L., Garnier, D. T., Kesner, J., Mauel, M. E., and Woskov, P., Nature Physics **6** (2010) 207.

[9] Yoshida, Z., Mahajan, S. M., Mizushima, T., Yano, Y., Saitoh, H., and Morikawa, J., Phys. Plasmas **17** (2010) 112507.

[10] Saitoh, H., Yano, Y., Yoshida, Z., Nishiura, M., Morikawa, J., Kawazura, Y., Nogami, T., Yamasaki, M., Phys. Plasmas **21** (2014) 082511.

[11] Furukawa, M., Phys. Plasmas **21** (2014) 012511.

[12] Rice, J. E. and Chamberlain, K. L., Phys. Rev. **A38** (1988) 1461.

[13] Goeler, S. VON., Stodiek, W., Eubank, H., Fishman H., Grebenshchikov, S., Hinnov, E., Nucl. Fusion **15** (1975) 301.

[14] England, A. C., Eldridge, O. C., Knowlton, S. F., Porkolab, M., Wilson, J. R., Nucl. Fusion **29** (1989) 1527.

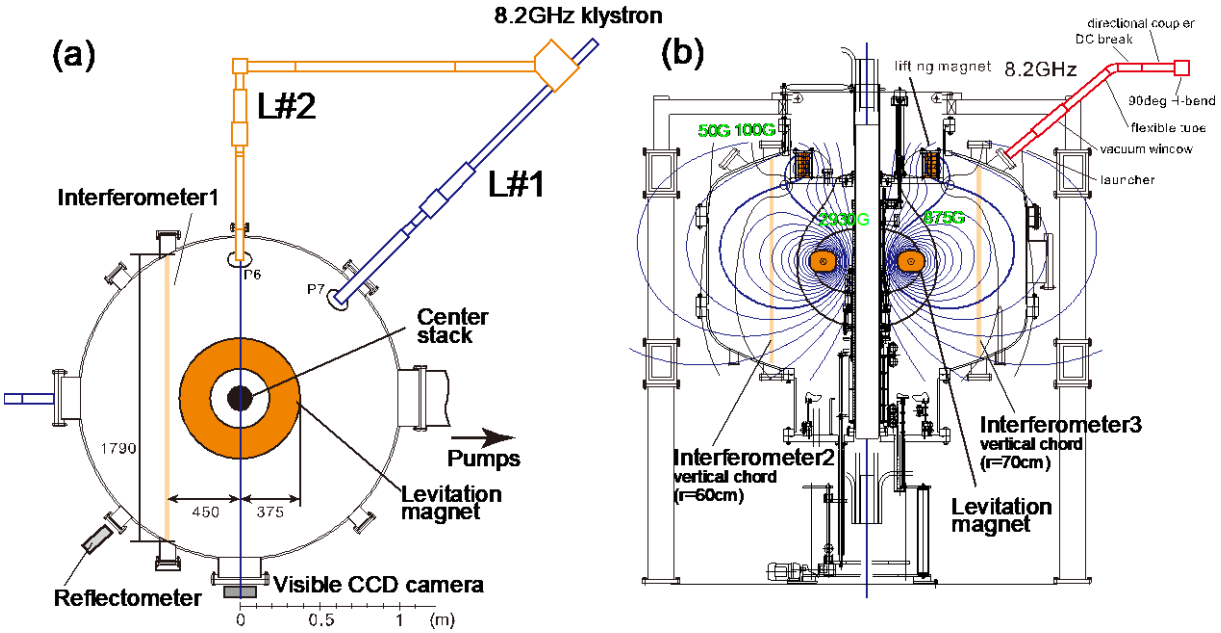

Fig. 1 (a) Top and (b) cross sectional views of RT-1. The transmission lines L#1 and L#2 for 8.2 GHz ECRH, resonance layers, and three interferometer cords are shown.

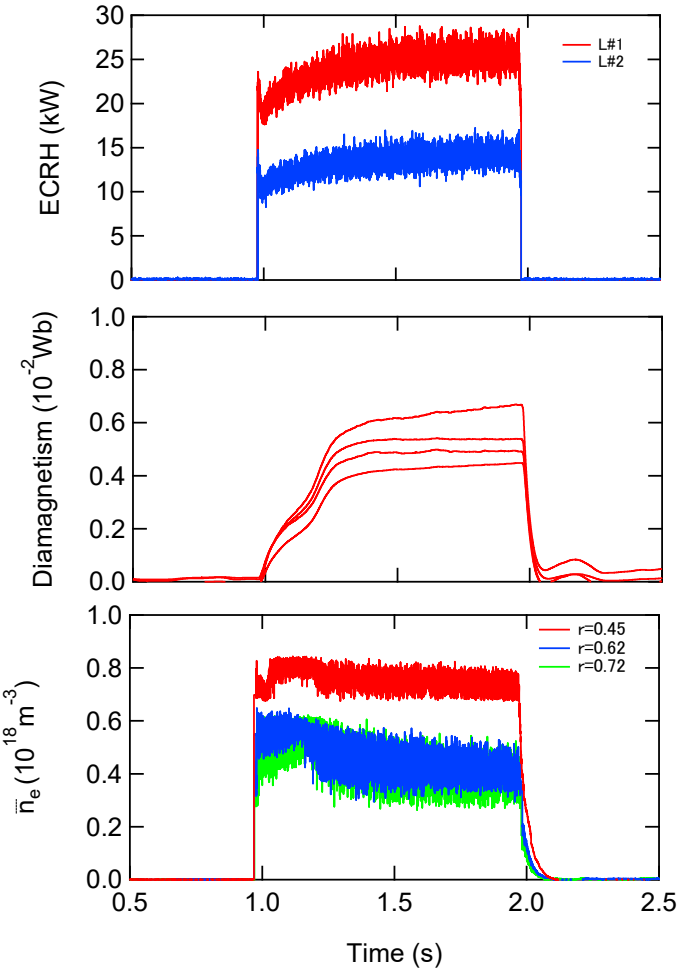

Fig.2 Discharge waveforms for high β deuterium plasma. (a) ECRH power, (b) diamagnetic signal, and (c) line average densities measured by interferometers.

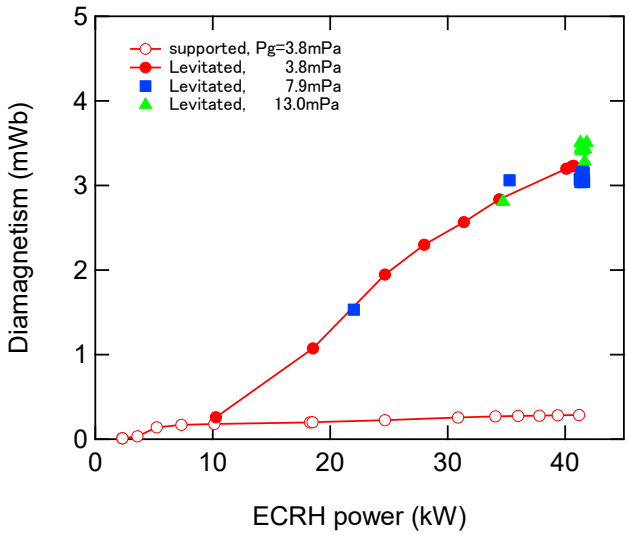

Fig.3 Diamagnetic signal as a function of ECRH power in H plasma of RT-1.

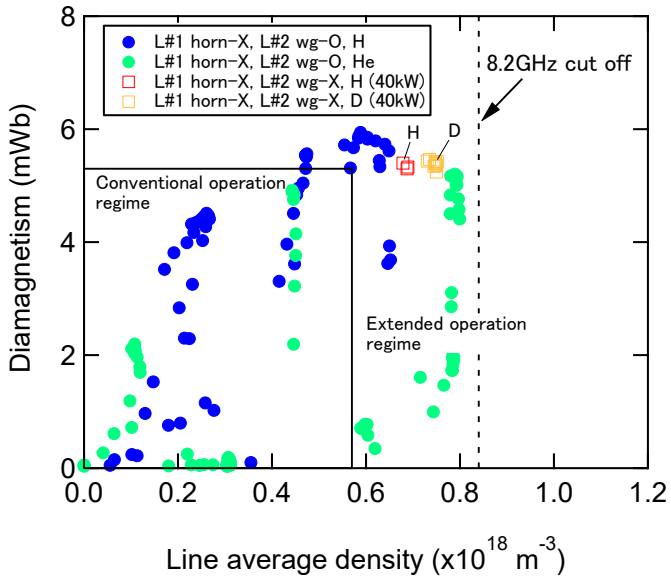

Fig.4 Extended $\bar{n}_e$ *and* W_p *for H, D, and He plasmas in the dipole configuration by the levitated superconducting coil of RT-1. The conventional and extended operational regimes are separated by lines. The broken line corresponds to the cutoff density for 8.2 GHz. H and D in the figure are the cases for the ECRH power of 40 kW for the comparison of isotope effect.*

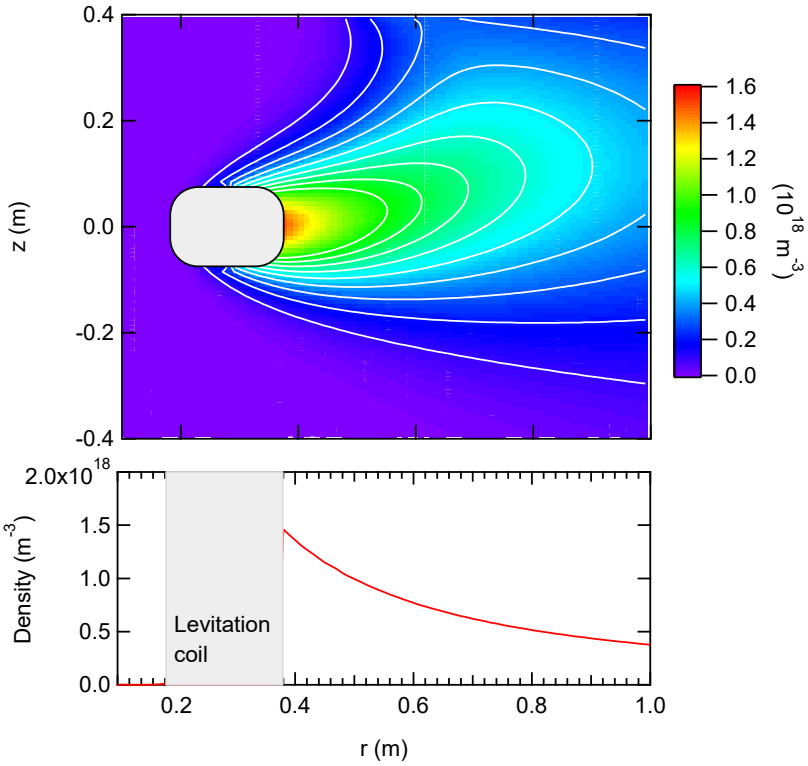

Fig.5 The electron-density profile in RT-1, which is reconstructed from three chord interferometer data. The lower graph shows the density profile at z = 0.

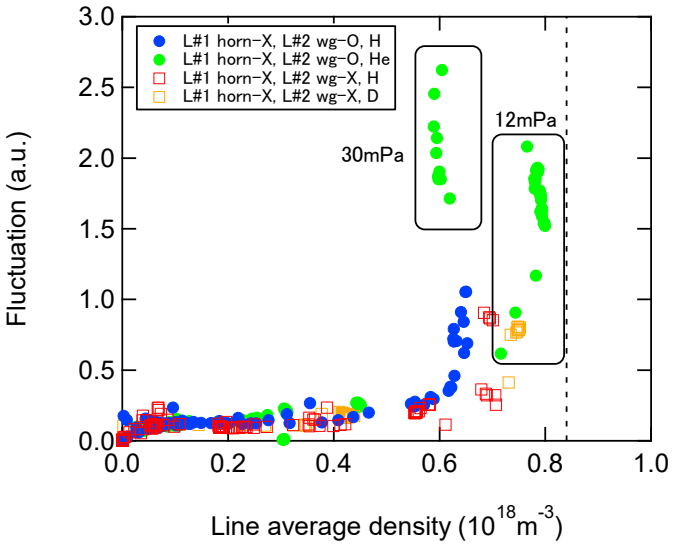

Fig.6 Dependence of the density fluctuation measured by the reflectometer on line average density in RT-1. The numbers in the figure indicate the helium gas pressure of 12 mPa and 30 mPa.

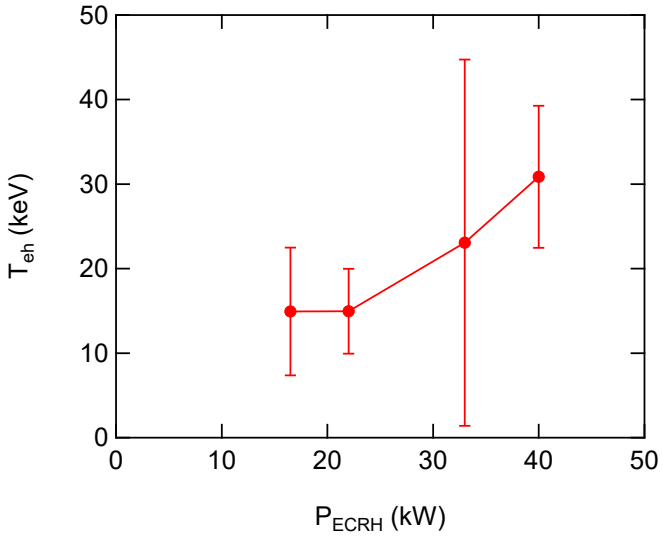

Fig.7 Electron temperature obtained from x-ray spectra as a function of ECRH power in hydrogen plasmas. The gas pressure is 7.6 mPa.

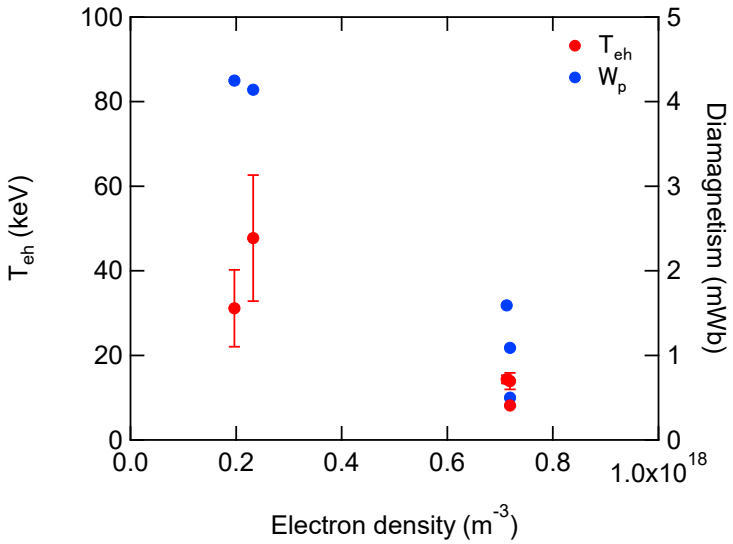

Fig.8 Electron temperature obtained from x-ray spectra and diamagnetism as a function of electron density in helium discharge. The filling helium gas pressure was increased to increase the electron density.